Lightning Protection for the AERA Preamplifiers

von

Tim Enzweiler

Bachelorarbeit in Physik

vorgelegt der
Fakultät für Mathematik, Informatik und Naturwissenschaften
der
Rheinisch-Westfälischen Technischen Hochschule Aachen

im August des Jahres 2010

angefertigt am

III. Physikalischen Institut A

Gutachter und Betreuer

Prof. Dr. Thomas Hebbeker
III. Physikalisches Institut A
RWTH Aachen

Contents

1 Introduction **1**

1.1 Cosmic Rays 2

1.1.1 Energy Spectrum of Cosmic Rays 2

1.1.2 Extensive Air Showers 3

1.2 The Pierre Auger Observatory 4

1.2.1 The Surface Detector 4

1.2.2 The Fluorescence Detector 5

2 Radio Detection of Ultra High Energy Cosmic Rays **7**

2.1 The Auger Engineering Radio Array 9

3 Lightning **11**

3.1 Formation of Thunderstorms 11

3.2 Cloud-Earth-Lightning 12

4 Requirements of Lightning Protection **15**

4.1 Power Rating of the Low Noise Amplifier 15

4.2 Coupling Lightning into the System 16

5 Possible Realisations of Lightning Protection **17**

5.1 Fine Protection 18

5.1.1 Schottky Diode 18

5.1.2 Zener Diode 19

5.2 Middle Protection 19

5.3 Coarse Protection 19

6 High-Voltage Test Techniques **21**

6.1 Norm for High-Voltage Test Pulses 21

6.2 Special Test Technique for Fine Protection 21

7 Testing Middle Protection **25**

7.1 Testing Gas Discharge Tube 25

8 Testing Fine Protection **27**

8.1 Surge Pulse 27

8.2 Schottky Diode BAT82 27

8.3 Zener Diode 1N5333B 28

8.4 Schottky Diode 1N5820 29

8.5 Testing Fine and Middle Protection 30

8.5.1 Zener Diode and GDT 30

8.5.2 Schottky Diode and GDT 31

9 Impedance Matching **33**

9.1 Test of the Impedance Matching 33

9.2 GDT 33

10 Conclusion and Outlook **37**

References **42**

Acknowledgements **43**

1. Introduction

Ever throughout the existence of man the observation of the sky has been of vital importance for the human race. The explanations of sky observation posed enormous difficulties. Thus, the phenomena observed, were often explained in religious rather than in scientific terms. Of course, quite a few phenomena were (and probably still are) totally unknown and could not be noticed at all.
Only with the gradual upcoming of science, explanations became seemingly possible. Especially in the 20th century considerable progress was made. On the other hand a lot of problems still have to be solved and a lot of questions have not even been asked yet.
One of these problems is the occurrence and the origin of Ultra High Energy Cosmic Rays (UHECRs), discovered some 90 years ago. Ever since then the origin and acceleration mechanism have been the subject of scientific research. Cosmic rays can develop energies above 10^{20}eV. When such a cosmic particle enters the atmosphere of the Earth and hits an oxygen or nitrogen atom a cascade of millions of secondary particles occures known as an "extensive air shower" (EAS).
Today's most important experiment with the largest detector area observing EASs is the Pierre Auger Observatory close to Malargüe in the province of Mendoza, Argentina.
Here, UHECRs are studied by employing a grid of more than 1600 water Cherenkov detectors on the ground in combination with fluorescence light telescopes which makes the Pierre Auger Observatory the only hybrid experiment so far.
A third form of detecting and studying UHECRs which came up in the 1960s has recently been reintroduced at the Pierre Auger Obersatory: The detection of air showers by measuring electromagnetic waves emitted at frequencies in the radio regime. This method seems to be quite promising for it is expected to be less expensive than other methods and gives calorimetric information of the air shower combined with a higher duty cycle compared to fluorescence detectors which can only measure fluorescence light of EAS during moonless nights.
To keep up the high duty cycle of the antenna stations their downtime due to damages caused by lightnings should be keept as low as possible. The aim of this thesis is the development and test of a lightning protection system for the preamplifiers of the radio antennas. The first two chapters will introduce the Pierre Auger Observatory and the mechanism the radio detection is based on. Chapter 3 gives a brief introduction in the field of lightning research. Chapter 4 and 5 show the requirements of a lightning protection system for the preamplifier and explain how this might be achieved. As one also has to test the lightning protection, in chapter 6 the reader is informed about test techniques for lightning protection. The next

three chapters contain the experiments of several lightning protection components. After this the last chapter gives a resumé about the prospects and problems for a preamplifier lightning system.

1.1 Cosmic Rays

It was in 1896 when A. H. Becquerel's discovery of radioactivity seemed to solve the problem that every statically charged body loses its charge over time. However, 16 years later it was Victor Hess with one of his famous balloon experiments who showed that the loss of charge of a body due to air ionization increases with altitude. According to this, at least some part of the continuous air ionization must be induced by extraterrestrial sources. This was the discovery of cosmic rays.
In 1938 Pierre Auger and Ronald Maze experimented with a grid of particle detectors. They frequently registered particles in coincidence despite the distance of a few meters between the detectors. This indicated that the observed particles are secondary particles of a common origin. This was the discovery of cosmic ray induced air showers.

1.1.1 Energy Spectrum of Cosmic Rays

The measured spectrum of cosmic rays today reaches from 10^8 eV to energies higher than 10^{20} eV. Cosmic rays with energies larger than 10^{18} eV are referred to as UHECRs. As shown in fig. 1.1 the differential flux of the cosmic rays approximately follows a power law,

$$\frac{d^2\Phi}{dEd\Omega} \sim \left(\frac{E}{GeV}\right)^{-\gamma}, \tag{1.1}$$

where the spectral index γ is approximately 2.7. In the range between $10^{15.5}$ eV and $10^{18.5}$ eV the spectral index changes to 3.1. These two discontinuities in the spectrum are known as 'knee' and 'ankle'. To understand the ankle feature is one of the aims of the Pierre Auger Observatory. The questions referring to the origin, the acceleration mechanism, the propagation in space and the chemical composition of UHECRs are also of great interest.

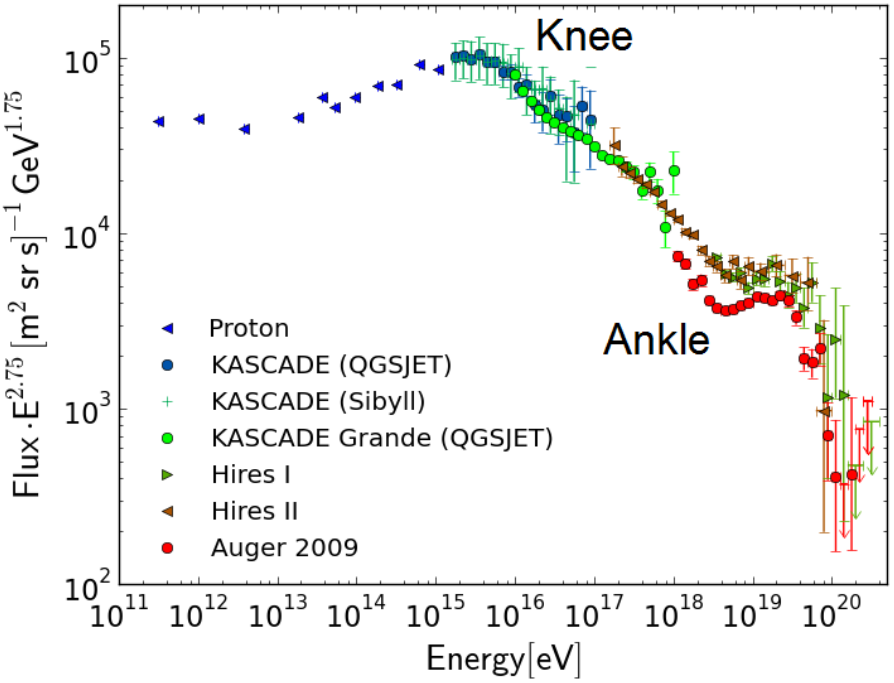

Figure 1.1: Measured spectrum of cosmic rays. In the plotted range the spectrum shows a power-law behavior. There is a change in the slope at the knee ($10^{15.5}$ eV) and at the ankle ($10^{18.5}$ eV). The integrated flux at the ankle is about 1 cosmic ray per km^2 per year. PROTON[1], KASCADE[2], KASCADE Grande[3], Hires I, II[4], Auger [5]

1.1.2 Extensive Air Showers

When UHECRs hit the atmosphere of the earth they interact with molecules of the air and produce in a series of reactions millions of secondary particles. These secondary particles approach the earth in form of a disk perpendicular to the main shower axis. This shower disk has a dimension of several kilometers when it reaches the surface of the earth but its thickness is only a few meters.
The first interaction takes place about 20 km above the surface of the earth and starts a hadronic shower consisting mainly of pions and a few kaons. They again hit molecules of the air and produce a hadronic shower. If not, after $\sim 10^{-8}$ s the $\pi^{\pm}$ and $K^{\pm}$ decay typically into muons and the corresponding neutrinos. For kaons the decay into pions is also allowed. Much more important for radio detection as shown in chapter 2 is the decay of the π^0 primarily into two photons after 10^{-17} s. These photons are the start of the electromagnetic cascade. They will decay into electrons and positrons by pair production. These again will produce photons by bremsstrahlung.

1.2 The Pierre Auger Observatory

The Pierre Auger Observatory is the largest experiment for observing UHECRs. It will consist of one observatory in the northern hemisphere in Lamar, Colorado, USA and one in the southern hemisphere in the province of Mendoza in Argentina. This allows to observe the whole sky. While the northern observatory is still in the state of planning, the southern observatory is completed and has already been taking data since beginning of 2004. It covers an area of ~ 3100 km^2 and consists of two complimentary detector systems: The Surface Detector and the Fluorescence Detector.

1.2.1 The Surface Detector

The Surface Detector (SD) consists of 1600 water Cherenkov detectors arranged in a hexagonal grid on an area of 3100 km^2. A station as shown in fig. 1.2 is filled with $12m^3$ ultra-pure water. Secondary particles crossing a SD station with a velocity faster than the speed of light in water emit Cherenkov light. This light is reflected on the specular inner surface and detected by three photo multipliers at the ceiling. As soon as at least four stations coincidentally detect particles, the data is acquired. The number of detectors hit by secondary particles depends on the energy and mass of the initial particle and on the geometry of the shower.

Figure 1.2: Surface detector station [6]

1.2.2 The Fluorescence Detector

On the way down to the Earth's surface secondary particles of the air shower excite nitrogen molecules in the air which emit fluorescence light by deexciting. This fluorescence light is measured with fluorescence telescopes. Therefore optimal conditions are required: Moonless and rainless nights. This leads to a low duty cycle of only 13 %.
Four buildings, each hosting six fluorescence telescopes, form the Fluorescence Detector (FD). Each building covers an azimuth angel of 180° and a zenith angel of 30°. The buildings of the FD are positioned around the SD-array (see fig. 1.3). In this manner they survey the air above the whole SD-array.

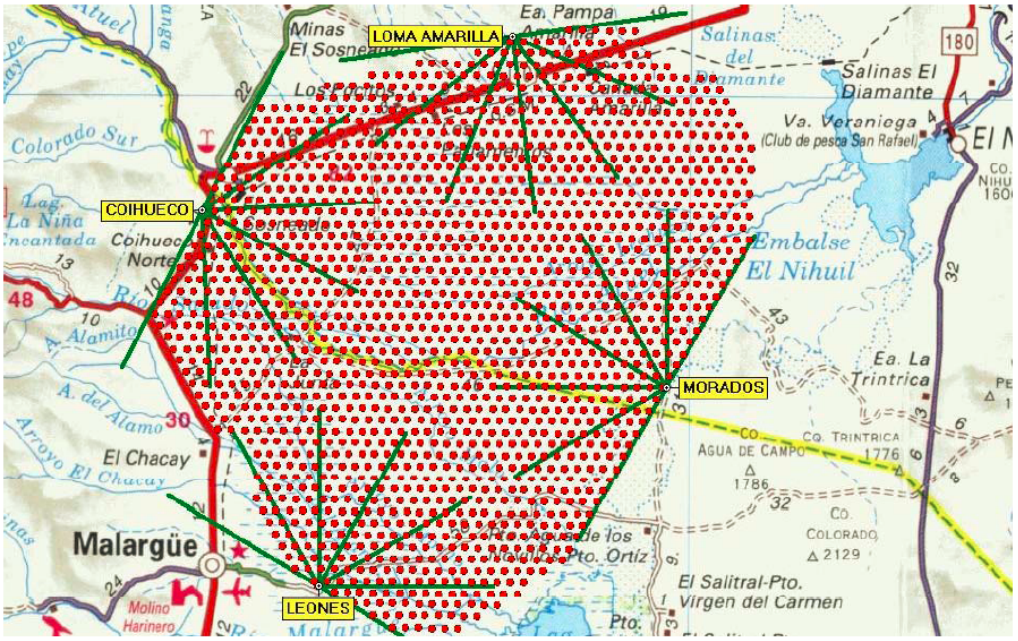

Figure 1.3: A schematic view of the southern site of the Pierre Auger Observatory. The red dots indicate the location of the water Cherenkov detectors. More than 1600 of these detectors arranged in a hexagonal grid build the Surface Detector. The green lines mark the viewing angles of the six fluorescence telescopes in each building. Together the 4 Fluorescence Detector buildings survey the air above the whole SD-array. [7]

2. Radio Detection of Ultra High Energy Cosmic Rays

A rather new method to detect UHECRs is based on the fact that extensive air showers produce radio emission. Actually in the 1960s first experiments measured such radio pulses in coincidence with Geiger counters [8]. However, at that time other techniques for detecting cosmic particles seemed to be more promising. In the early 2000s the interest in radio detection was renewed, due to new models to describe radio emission and of course, the technological progress. In fact the radio detection offers several advantages over FD and SD. Contrary to FD the radio detection has no limited duty cycle. As the emitted radio waves form a coherent pulse, that is formed during the whole development of the shower, the radio pulse contains information about the shower development in the atmosphere.

The 'coherent geosynchrotron emission'-model from Huege and Falcke [9] is the at present most-established approach to explain the radio emission of extended air showers (EAS).
A charged particle of the EAS which moves through the magnetic field of the Earth is deflected by the Lorentz force to a curved track. It is also well known, that a particle with charge q and mass m on a curved track emits synchrotron radiation. So do the particles of the EAS. The power of synchrotron radiation is given by [10]

$$P = \frac{2}{3}\,\frac{q^2 c}{r^2}\,\beta^4\,\gamma^4 \quad \text{, with} \quad \beta = \frac{v_\perp}{c} \quad \text{and} \quad \gamma \approx \frac{E}{m}\,, \tag{2.1}$$

where $v_\perp$ is the velocity of the particle perpendicular to the axis of rotation, E is the energy of the particle and r is the gyro-radius of the particles caused by the magnetic field. The gyro-radius is given by

$$r = \frac{\gamma\, m\, v_\perp\, c}{q\,|\vec{B}|}\,. \tag{2.2}$$

Inserting (2.2) in (2.1) yields

$$P = \frac{2}{3}\,\frac{q^4}{m^4\,c^5}\,v_\perp^2\,E^2\,B^2\,. \tag{2.3}$$

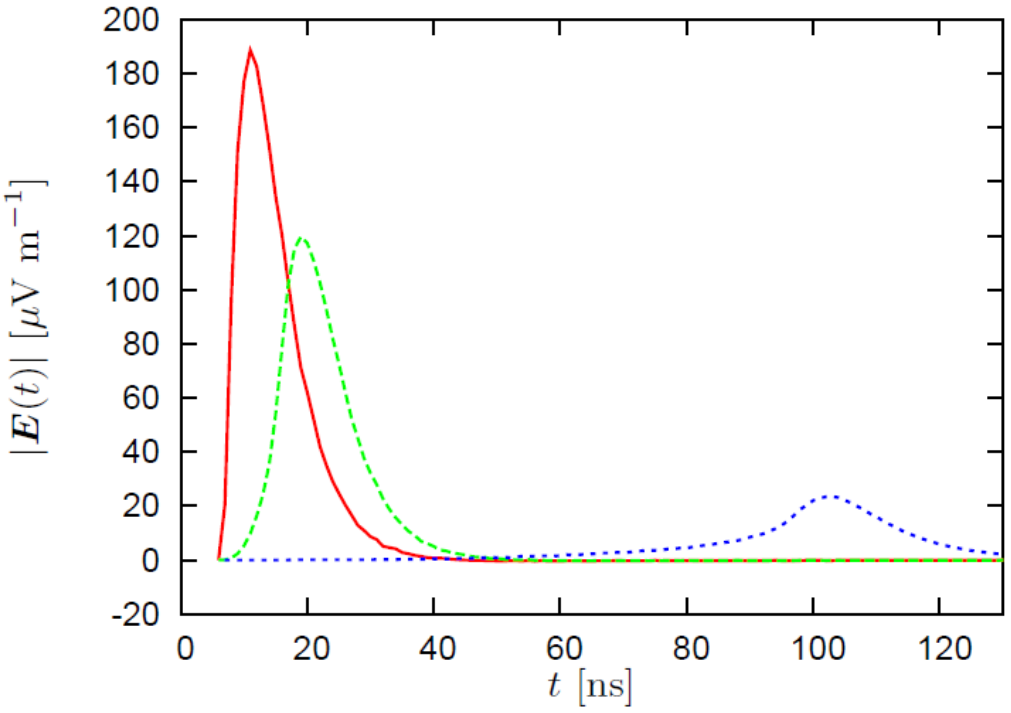

Figure 2.1: Simulated time-dependence of the raw pulses originating from the shower maximum as observed by an observer at 20 m (red solid line), 140 m (green dashed line) and 460 m (short dashed line in blue) to the North from the shower center.[11]

According to this the radiated power

$$P \sim E^2 \quad \text{and} \quad P \sim m^{-4} \,. \tag{2.4}$$

Since the radiated power is proportional to the fourth power of the inverse mass the only particles giving a non-negligible contribution to the emitted radiation are electrons and positrons. All other particles produced in the shower are much heavier. Thus, the electromagnic cascade is the subject of interest when studying radio emission.
Huege and Falcke simulated radio emission from cosmic ray induced air showers [11]. As shown in fig. 2.1 the electric field of an EAS can only be observed near the place where the shower reaches the ground. The distance between the particles is small compared to the wavelength of the radio emission, since the particles of the shower propagate within a thin disc. Hence, the permanent emission during the propagation of the air shower results in a superposition to a coherent radio pulse.

In 1970, Allan was able to parameterize the amplitudes of the measured radio pulses [12]. The amplitude of the electric field ϵ_ν at a certain frequency ν depending on the primary particle energy E_p, the angle between the shower axis and the magnetic field

of the Earth α and the zenith angle θ between the shower axis and the perpendicular distance R from the shower axis to the obserever is given by

$$\epsilon_\nu = 20 \cdot \left(\frac{E_p}{10^{17}\ \mathrm{eV}}\right) \sin\alpha\ \cos\theta\ \exp\left(-\frac{R}{R_0(\nu,\theta)}\right) \mu\mathrm{V\ m^{-1}\ MHz^{-1}}\ \ [13]. \qquad (2.5)$$

The distance-dependent exponential damping involves the attenuation parameter R_0. Recent results from the LOPES experiment determine it to $R_0 = (230 \pm 31)$ m [14].

2.1 The Auger Engineering Radio Array

The radio detection technique seems to be a very promising way for air shower detection. Thus, due to the results of several small test setups at the Auger Observatory area the collaboration decided to build the *Auger Engineering Radio Array* (AERA) in 2009.
AERA will consist of 160 detector stations. They will be arranged in a triangular grid in an area of $\sim 20\ \mathrm{km}^2$ at the existing observatory. This makes it possible to measure events in coincidence with the FD and the SD.
The sensitive part of each station which is schematicly shown in fig. 2.2 is an antenna with a *low-noise amplifier* (LNA) with filter directly mounted at the antenna. The output of the LNA is connected to the analogue signal processing consisting of two times filter plus high gain amplifier. From there the signal goes to the digital signal processing where it is converted to digital by an *analogue to digital converter* (ADC). This is needed for the trigger unit. The last part is the COMMS system which works on WLAN. It transfers the data to the central radio station (CRS); but not all, only if a certain number of detector stations trigger at once. Therefore the COMMS system just sends the information that it has triggered and only if the CRS demands more information, the data it is sent.
First data acquisition of AERA is schedueled for this autumn (2010). One point to keep the stations operating is to prevent a breakdown caused by lightning. Before the design of a suitable protection is discussed the following chapter gives a short general introduction to thunderstorms and lightning.

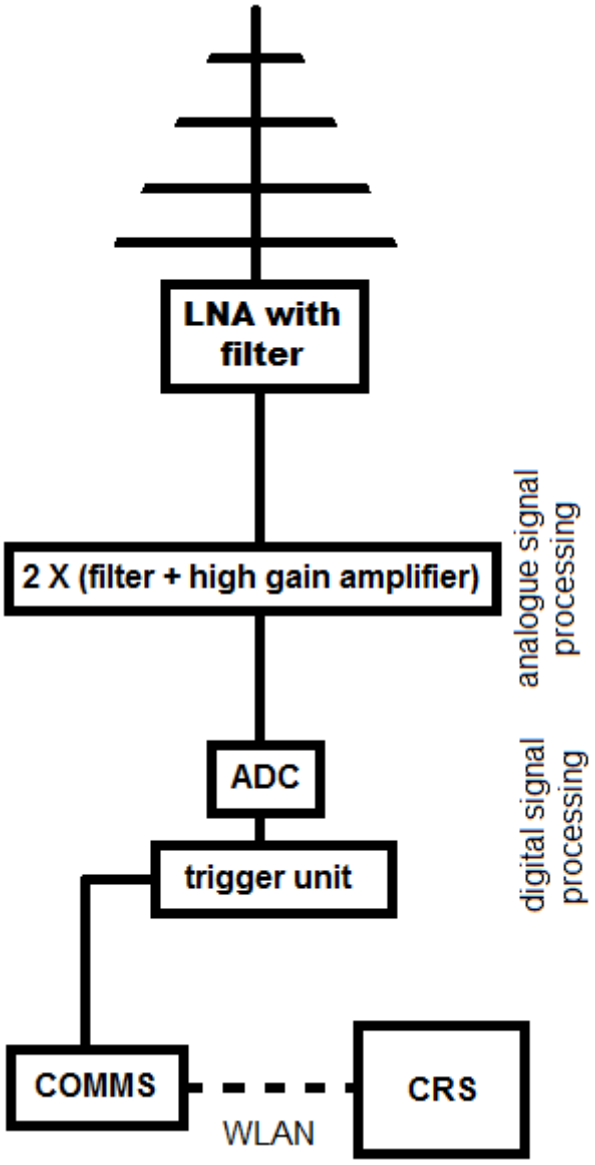

Figure 2.2: Schematic set-up of the detector station and CRS.

3. Lightning

Lightning research is a wide field with a lot of unsolved problems and questions. This chapter just gives a little insight into the field of lightning science and makes no claim to be complete.
As shown in fig. 3.1 the area around the Auger Observatory is hit by a not negligible number of lightnings.

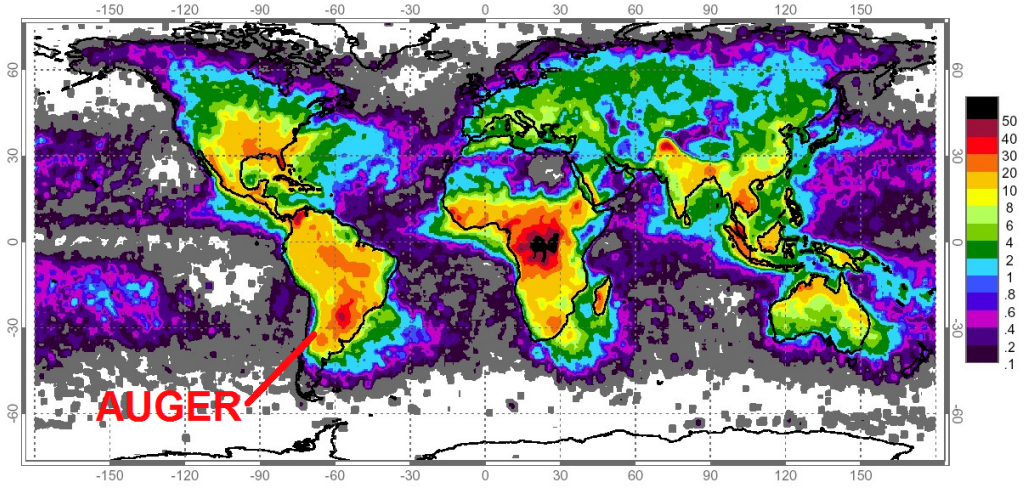

Figure 3.1: Data from space-based optical sensors reveal the uneven distribution of worldwide lightning strikes, with colour variations indicating the average annual number of lightning flashes per km^2.[15]

3.1 Formation of Thunderstorms

A thunderstorm arises when masses of moisture are lifted upwards into the atmosphere by warm air. At higher altitude the temperature decreases and the moisture rapidly condenses to drops of water, which in turn appear as cumulus clouds. At the top of the cumulus cloud the temperature decreases to $-50°$ C and so the drops of water are forming ice crystals on their way up.
Lightning occurs when in big cumulus clouds large updrafts separate electric charge. The upper side of the cloud contains positively charged ice crystals and the lower side contains liquid drops of water which are negatively charged.
The electric field intensity between the Earth and the bottom side of the cloud can typically increase up to several 10 kV/m.

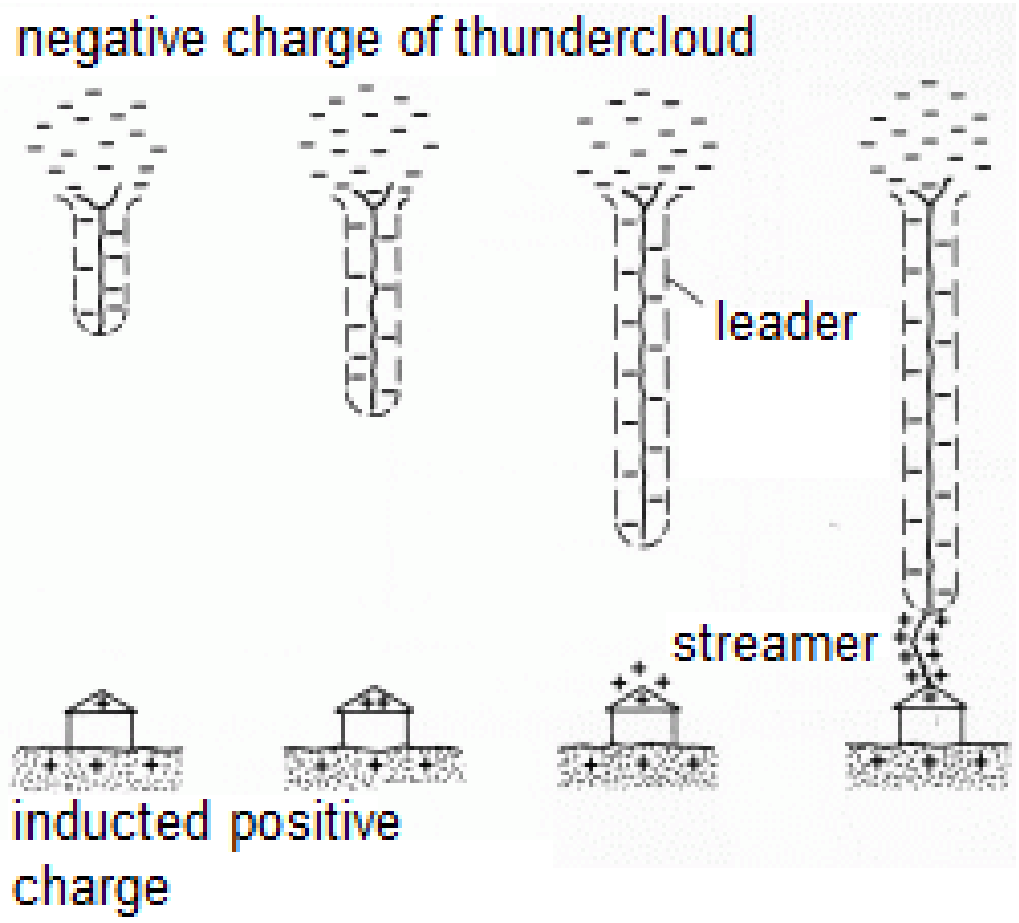

Figure 3.2: Developemet of a leader and a streamer[16]

3.2 Cloud-Earth-Lightning

95% of lightning is cloud to Earth lightning as illustrated in fig 3.2. The remaining 5% is Earth-to-cloud lightning. This appears only from very high points such as church steeple, and therefore only cloud-Earth-lightning is discussed.
The dielectric strength of air is about 3 MV/m, but the electric field during a thunderstorm hardly ever reaches more than 200 kV/m. The question why lightning occurs nevertheless under these conditions is subject of current research. One theory is that they are triggered by cosmic particles.

An initial discharge is a path of ionized air. It starts at a negatively charged region in the thundercloud. These ionized discharge channels are called *leaders* and have a diameter of 10 m with a highly ionized plasma core of 1 cm diameter. They proceed their way downwards in rather short steps of mostly 50 m to 100 m. When this leader approaches the positively charged ground, a conductive discharge, called *positive streamer*, runs from ground to the leader. Once a continuous channel of ionized air from ground to cloud is established, this becomes a path of least resistance; which allows various *return strokes* with a much stronger current.
The whole lightning from the initial discharge to the last return stroke can take

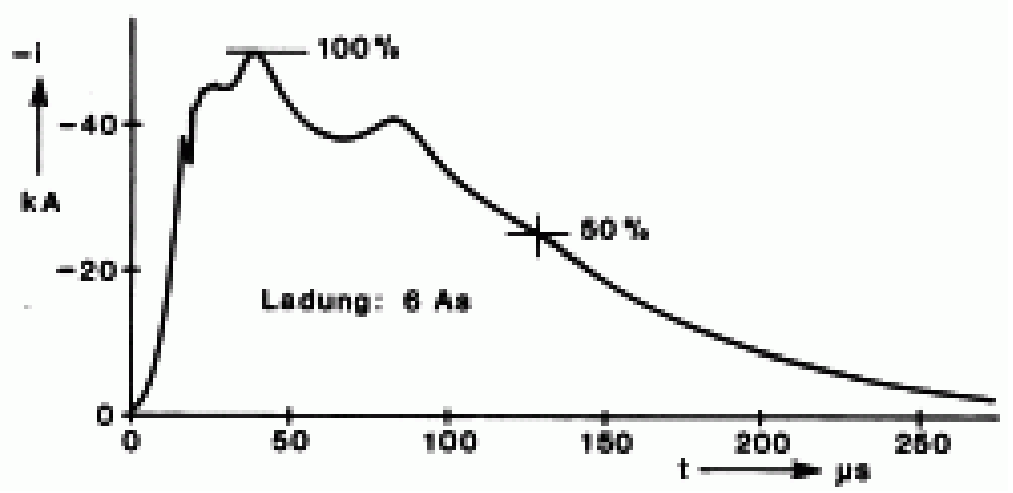

Figure 3.3: Time-dependent current of an over-average return stroke. [16]

up to 1 s whereas single strokes are much shorter: The several steps of the leader propagate with a speed of 300 km/s and between the steps there is a pause of a few 10 μs. Once the channel is built up the electric charge in it is conducted to the Earth in 10 μs to 300 μs. So the whole initial discharge takes about 20 ms.
The initial discharge is followed by several return strokes with time intervals of 10 ms to a couple of 100 ms.

As visible in fig. 3.3 the maximum current of a return stroke goes up to several 10 kA in a few 10 μs. There are up to about 40 discharges at one lightning. Concerning AERA: If a lightning strikes directly into an antenna the whole detector station will be destroyed; but also lightnings that do not directly strike into an antenna can be dangerous as we will see in the next chapter.

4. Requirements of Lightning Protection

4.1 Power Rating of the Low Noise Amplifier

Within this thesis a lightning protection is developed to protect the preamplifier designed for AERA by M. Stephan [17]. This low noise amplifier (LNA) has a power gain of about 22 dB at a working frequency range from 30 MHz to 80 MHz [17]. Interesting is the maximum permissible voltage U_p. This doubtlessly depends on the form of the pulse. The second question is whether U_p is dependent on the direction (input/output) of the surge pulse reaching the LNA.
M. Stephan showed that the amplifier resists continuous +5 dBm at the input. That means $P = 3.162$ mW at 50 Ω. Since $P = U \cdot \frac{U}{R}$ the voltage is $U \approx 40$ mV. As this is valid for continuous operating, much higher voltage for a short pulse is expected. So the LNA is tested with rectangular pulses up to 13 V like in fig. 4.1 to get a lower limit for the maximum permissible voltage U_p.

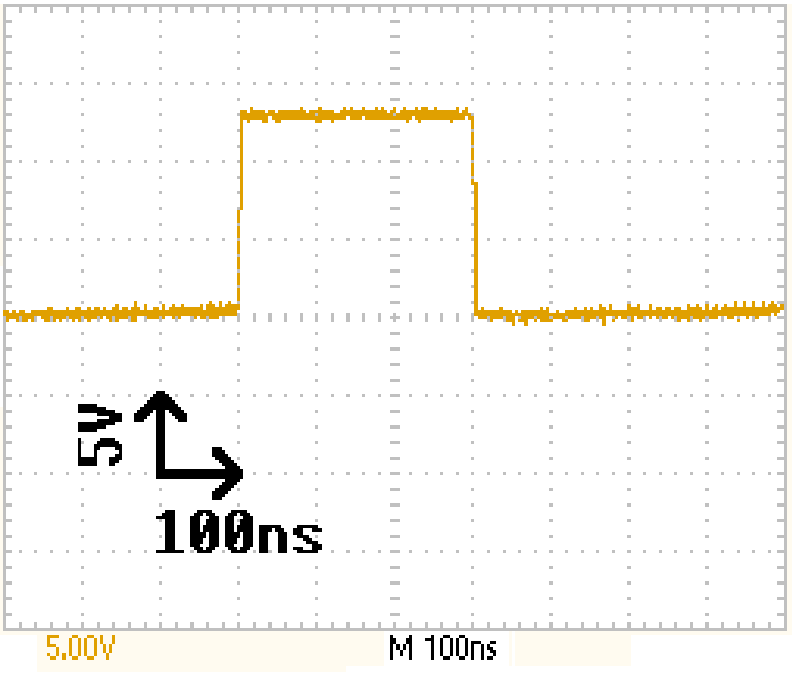

Figure 4.1: rectangular pulse for testing the limits of the LNA

To test the power rating at the input, the LNA is set up like in normal operating mode: Therefore the LNA is connected at its output by coaxial cable to a Bias-T. The Bias-T is necessary for the phantom powering of the amplifier. It supplies the signaling cable to the amplifier with about 6 VDC. The LNA itself regulates the voltage down to constant 5 V, which are needed for the transistor[1]. The input is connected to a rectangular pulse generator.
The pulse generator produces pulses with duration of 300 ns and a repetition time of 100 ms. The maximum voltage of the pulse starts at 0.25 V and is stepwise raised to 13 V. The step sizes are between 0.05 V at the beginning and 1 V at the end. The functional capability is tested with the network analyzer mode of he spectrum analyzer FSH4 from Rohde & Schwarz. The voltage is raised up to the maximum voltage of the rectangular pulse generator (13 V) and the LNA is not damaged by the pulse from fig. 4.1. This leeds to the conclusion that the lower limit $U_p \geq 13$ V.

4.2 Coupling Lightning into the System

There are three ways the high voltage of a lightning can couple to the detector station: capacitively, inductively and resistively. As the antenna is sensitive to capacitive and inductive coupling these two ways would imply that the high voltage is connected to the input of the LNA. The third possibility is that the high voltage couples resistively into the grounding of the system.
However, in the end it only matters whether the high voltage couples at the antenna or the electronic behind the output of LNA. Accordingly, the lightning protection has to be designed for the input, the output or both. This thesis is concerned with the protection of the input of the LNA. However, the results will be also helpful for protecting the output.

[1]The DC/DC-converter supplies the station with 6 V.

5. Possible Realisations of Lightning Protection

The basic idea for protecting the LNA in case of overvoltage is to shorten the input or output of the amplifier. This is dependent on the side at which the high voltage is connected to the amplifier.
For protecting the LNA a three-stage-system is planned: 'fine protection', 'middle protection' and 'coarse protection'.
The fine protection has to derate the voltage to a value less than U_p (see 4.1). The middle protection has to protect the damageable fine protection. The middle protection itself is protected by the coarse protection. A schematic of the whole protection system is shown in fig. 5.1. The three stages in detail are explained in the next sections.

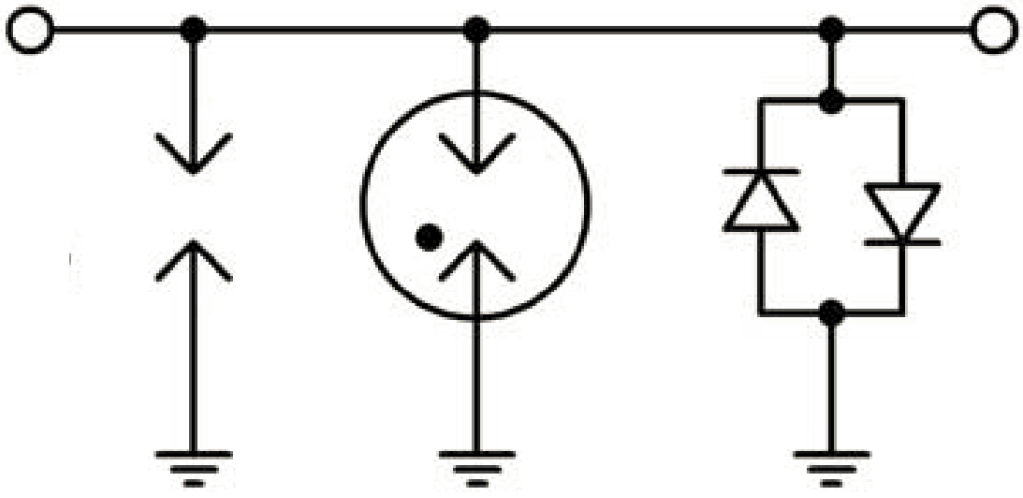

Figure 5.1: Schematic of the three-stage-system. From left to right: spark gaps (coarse protection), gas discharge tube (middle protection) and diodes (fine protection)

5.1 Fine Protection

The fine protection needs a very quickly responding behaviour on account of the rapidly rising voltage of a lightning strike. Here, fast switching diodes, like Schottky and Zener diodes, seem to be the first choice.

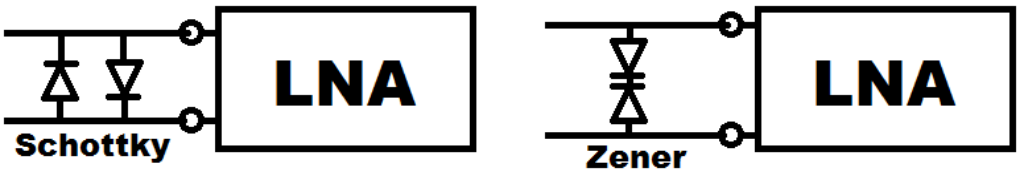

Figure 5.2: Schematics of the connection of Schottky and Zener diodes

5.1.1 Schottky Diode

Two Schottky diodes are connected parallel to each other like in fig. 5.2, so that - no matter if the pulse is positive or negative - one diode is connected in forward bias. In forward bias the current flow is exponential with the voltage and starts to become significant at the turn-on voltage U_{on}. At the working range of the amplifier which is marked in fig. 5.3 the voltage is always between the breakdown voltage U_{br} and U_{on}. But when a lightning appears the voltage quickly rises above U_{on} and therefore shortens the input.

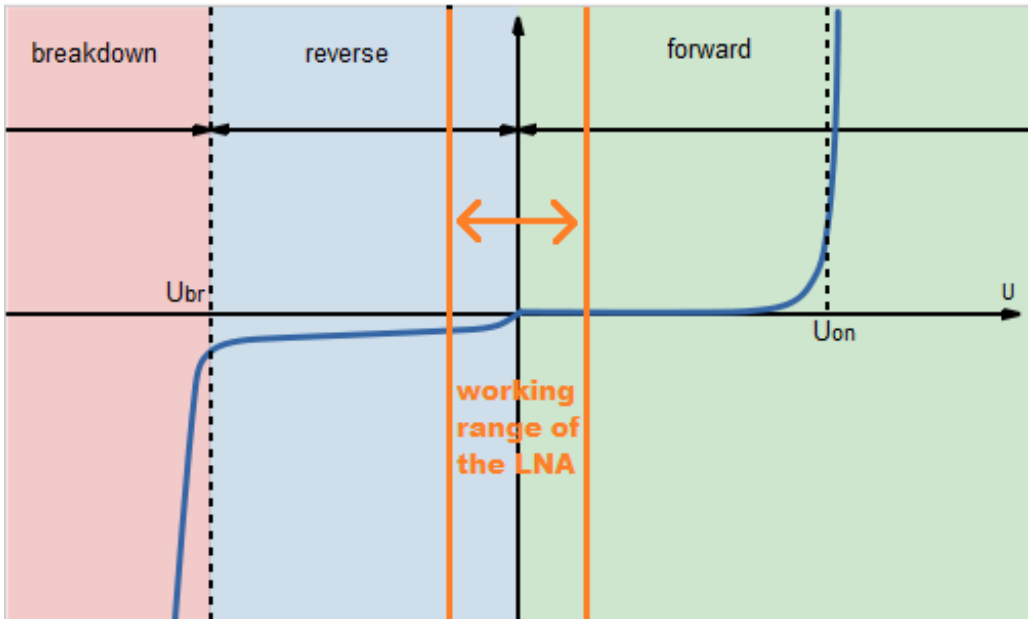

Figure 5.3: Current-voltage characteristic of a Schottky diode. Originally taken from [18]

5.1.2 Zener Diode

A Zener diode works in forward-bias like a normal diode; but if it is reversely biased it will allow a significant current below its Zener voltage U_z (breakdown voltage). This is caused by the heavily doped P-N junction of a Zener diode. Usually the energy bands of the P and N materials are on different levels, but the electric field caused by the reverse bias causes the valence band of the P material to overlap the conduction band of the N material. This allows electrons to tunnel from the valence band of the P doped material to the conduction band of the N doped material.
Two Zener diodes are connected against each other like in fig. 5.2 so that in normal operation mode always one diode is reversely biased. But when there is a surge pulse with a voltage larger than U_z, the diodes will keep the voltage down to U_z due to the Zener effect.

5.2 Middle Protection

The fine protection is indeed the most important stage of the lightning protection system, since only this stage is fast enough to protect the amplifier against the rapidly rising edge of a lightning-caused surge pulse. It is also the most vulnerable stage of protection. Thus the middle protection is needed to keep the current and so the power away from the fine protection. For this a gas discharge tube (GDT) is recommended. A tube filled with gas that ionizes and becomes conductive at a certain voltage. For this reason a gas discharge tube from Huber and Suhner which becomes conductive at a static breakdown voltage of 90 V is tested. For short pulses the breakdown voltage will be higher.

5.3 Coarse Protection

The coarse protection is needed when the voltage is too high for the middle protection. Therefore spark gaps seem to be a good option. They are fast and nearly indestructible. Their only disadvantage compared to GDT is their higher breakdown voltage.

6. High-Voltage Test Techniques

In the last chapter several possibilities for the different stages of lightning protection were discussed. Now one has to find out which of those is working best for the LNA. Therefore the lightning protection has to be tested. Depending on whether the whole protection system at once or just individual stages are tested the used test technique varies.
The whole system is normally tested by using a norm for high-voltage test techniques. For testing a single stage one just has to consider to stress the stage where it should work.

6.1 Norm for High-Voltage Test Pulses

The international standardization of electrotechnology is influenced by the International Electrotechnical Commission (IEC). The IEC-60 for high-voltage test techniques describes how to test lightning protection. The German DIN-Norm DIN 57432 and the VDE 0432 are identical with the IEC-60.
According to the IEC-60 a surge voltage or surge pulse is a transient aperiodical voltage which increases fast to its peak value and then slowly decreases to zero. The front-time duration T_f and the time to half-value $T_{1/2}$ are the characteristical parameters for this surge voltage. The shape of a typical test-pulse can be seen in fig. 6.1. The magnitude of the maximum voltage U_{max} is not defined in this norm. It only depends on the voltage the protection shall work against.

The best set-up to generate surge pulses conform to the IEC-60 is a Marx generator like in fig. 6.2. In a Marx generator a number of N capacitors C_s is charged in parallel to a certain voltage U_0, and then gets connected in series by spark gaps. With the approximation $R_e C_s \gg R_d C_b$ the voltage over C_b would be $U_b \approx N \cdot U_0 \cdot \frac{C_s}{C_s+C_b}$. The test item P is connected in parallel to C_b and tested with a voltage of U_b. The resistors R_d and R_e determine the shape of the pulse. A higher R_d reduces the *front-time duration* T_f as R_e does for the *time to half-value* T_f.
The Marx generator is the first choice for testing a whole lightning protection system at a high voltage, but as the construction of a Marx generator takes a lot of time it is not used in this work.

6.2 Special Test Technique for Fine Protection

The fine protection is the first reacting stage. Therefore quick responding behaviour has to be tested by a pulse with very rapidly rising edge. A test pulse according to the IEC-60 with a maximum voltage of only a few hundred volts would according

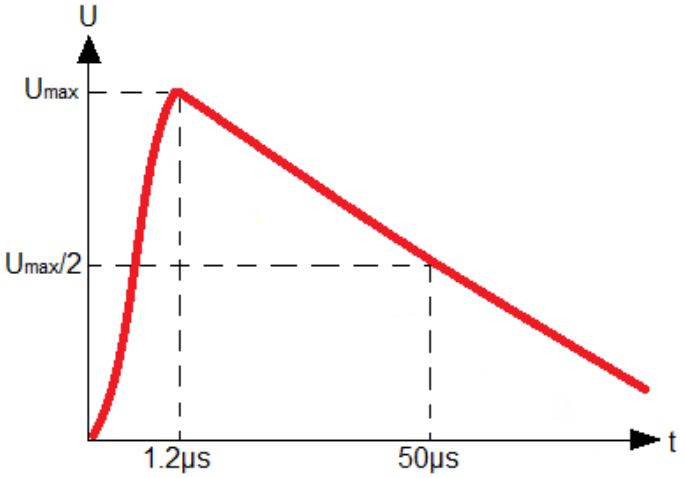

Figure 6.1: The shape of a pulse due to IEC-60, where U_{max} is the maximum voltage against the protection should work. The *front-time duration* should be $T_f = 1.2\ \mu s \pm 30\%$. The *time to half-value*, is defined as $T_{1/2} = 50\ \mu s \pm 20\%$

to its shape have a rather slow rising edge. Therefore we are going to use a quasi rectangular pulse with a voltage rising as fast as it does in a $U_{max} = 24$ kV test pulse in accordance with the IEC-60. That results in a rising voltage speed of 20 kV/μs. Pulses rising faster than this would also be acceptable.

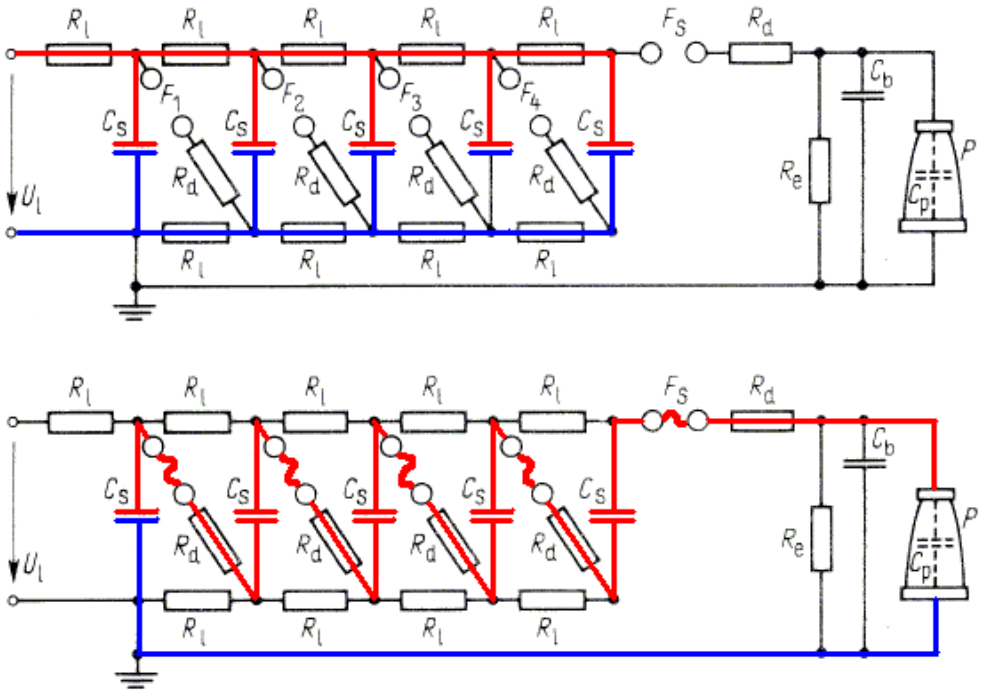

Figure 6.2: Schematics of a Marx generator for generating high voltages. Top: All condensators are charging in parallel. Bottom: All condensators connected in series by spark gaps. Taken from [19].

7. Testing Middle Protection

As announced in chapter 5.2 the gas discharge tube (GDT) 9071.99.0548 from Huber and Suhner is going to be discussed in this chapter. For testing the GDT a 500 V pulse is used. This pulse is generated with a 'Sprunggenerator' which was borrowed from the 'Institut für Hochspannungtechnik' at the RWTH Aachen University. The operating mode is not exactly known. Basically it charges a capacitor which discharge is triggered by a button to connect its voltage to 50 Ω at the output.
In fig. 7.1 a 500 V test pulse as well as the pulse after passing the GDT are shown. It is clearly visible that the gas in the GDT needs 350 ns to ionize.

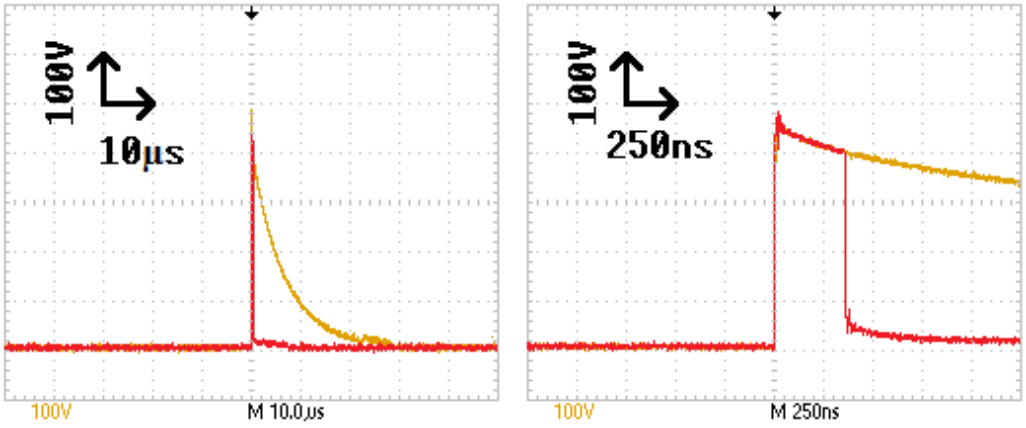

Figure 7.1: 500 V test pulse (*yellow*) for testing the GDT and residual pulse (*red*) when using GDT for protection. The right diagram shows the rising edge with a higher time resolution

7.1 Testing Gas Discharge Tube

To be sure that a fine protection is really needed, a test with just a GDT for protection is done. Therefore the 500 V test pulse like in fig. 7.1 is used. The LNA with the GDT at its input is connected to the surge pulse generator and the lightning protection is tested by a single pulse. Comparing the amplifier's gain before and after the test is a check for test fail. The gain is measured with the network analyzer mode of the spectrum analyzer FSH4. As visible in fig. 7.2 the LNA is fully functional before the test and fig. 7.3 shows that the amplifier is destroyed by the test pulse.

Thus, a fine protection is definitely required.

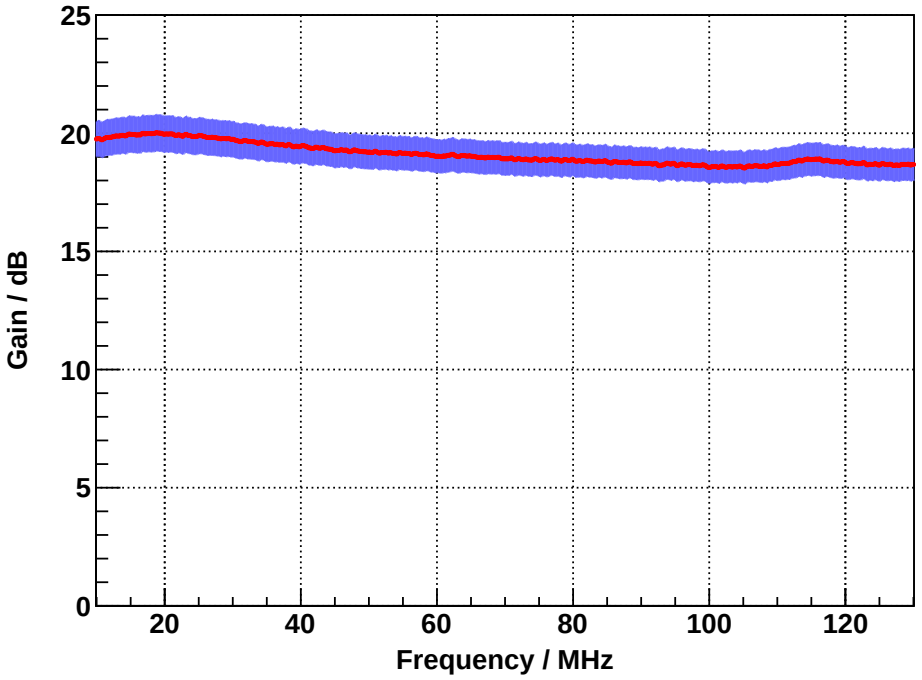

Figure 7.2: *Test-LNA-1*: Gain of a properly working amplifier. Systematical errors in blue.

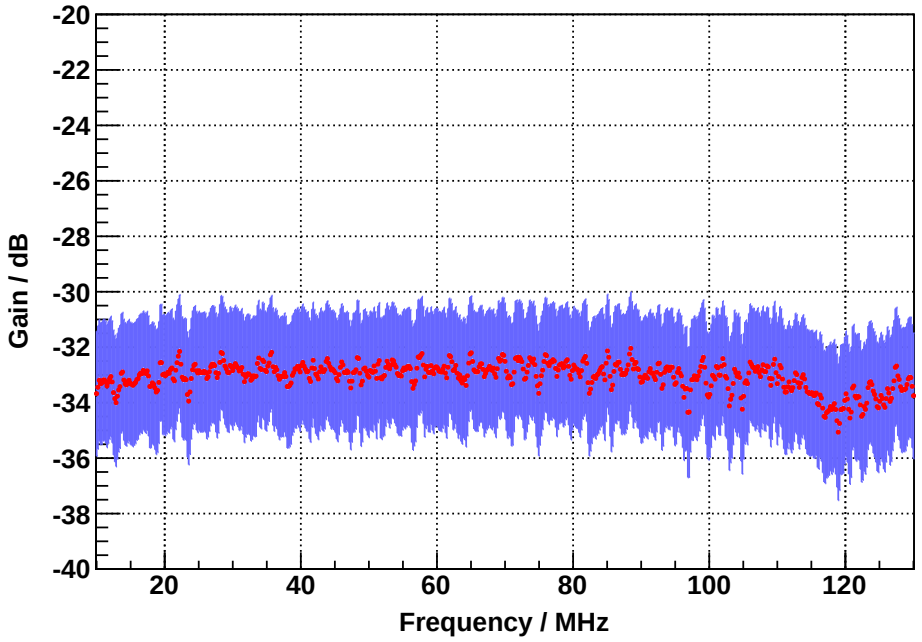

Figure 7.3: *Test-LNA-1* protected by a GDT(gas discharge tube). Gain after firing one 500 V pulse like in fig. 7.1 at its input. Systematical errors in blue.

8. Testing Fine Protection

8.1 Surge Pulse

The diodes represent the fine protection, and therefore they have to react extremely quickly. Thus a test pulse for the first stage requires a rapidly rising edge.
In order to generate this pulse with 50 Hz a capacitance has to be charged and then it has to be connect to the protection circuit by a relay. As capacitance 62 m RG58 C/U coaxial cable with a capacitance of 100 pF/m are used. The advantage of the cable compared to a capacitor is that its pulse has a very abrupt trailing edge. The voltage rises to 120 V in less than 6 ns.

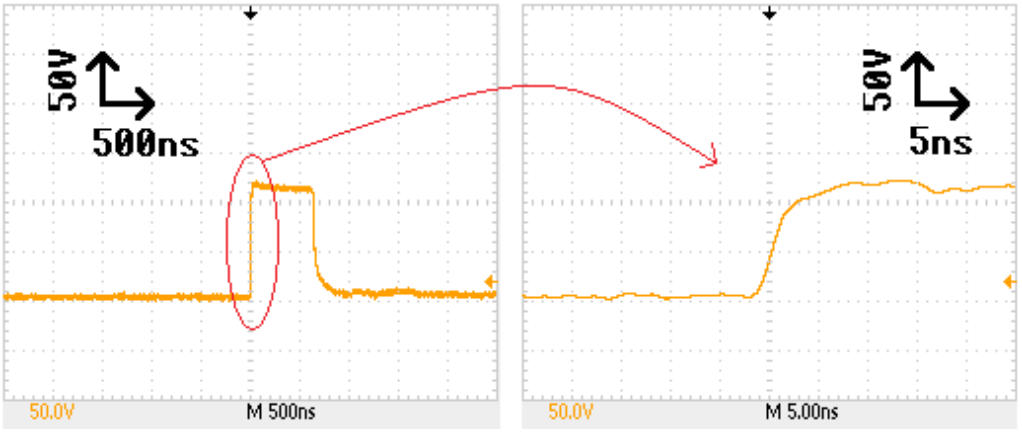

Figure 8.1: The test pulse without any protection. *Left*: The whole pulse. *Right*: The rising edge with a higher time resolution.

8.2 Schottky Diode BAT82

The BAT82 is a fast switching Schottky diode with a low forward voltage U_{on} = 410 mV (for U_{on} see section 5.1). These are good properties when trying to drop the voltage.
In order to test the Schottky diode BAT82 the set-up is constructed as in fig. 8.2. The pulse generator applies the voltage to 50 Ω. Due to the way the diodes are connected to ground, there is always one in conducting direction. Hence the voltage can be divert, no matter if the pulse is positive or negative. 10 Ω resistors are connected in series with each diode to protect it against too high current. Even though it reduces its ability to divert voltage, the current is required to conduct the electric charge to ground.
The 500 Ω resistor in combination with the 50 Ω at the input of the oscilloscope present a 10 : 1 voltage divider.

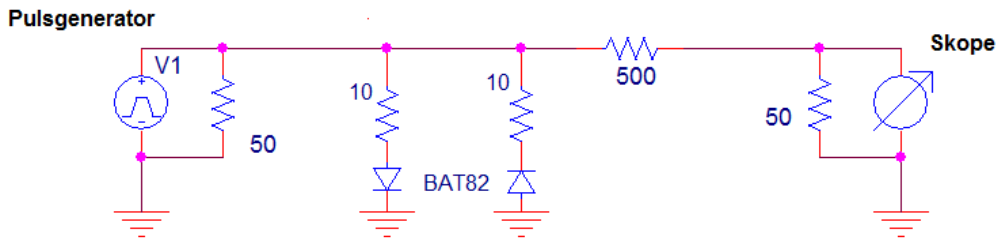

Figure 8.2: Test setup for the Schottky diode BAT82 with 10 : 1 voltage divider (500 Ω : 50 Ω). An additional 10 Ω resistor protects the diode from too much current.

As apparent from fig. 8.3 the BAT82 drops the voltage from 120 V to a residual voltage $U_{res} = 25$ V. The conspicuous oscillation can be attributed an impedance mismatch which leads to reflections of the pulse.

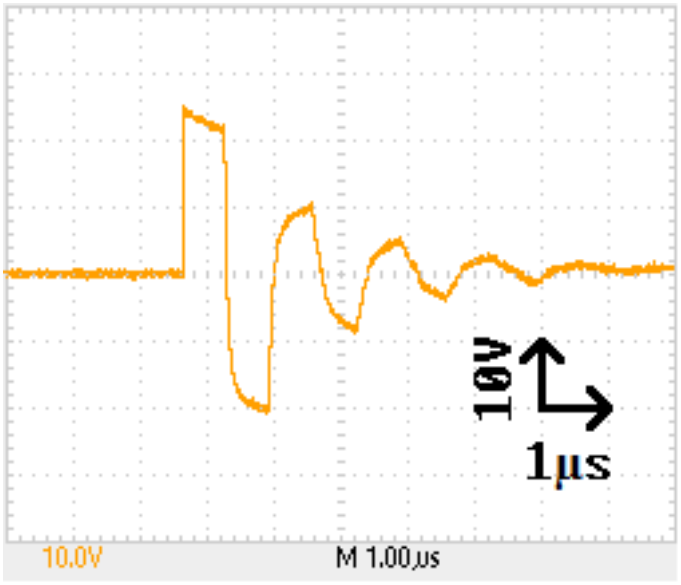

Figure 8.3: Pulse measured at the scope with configuration as in fig. 8.2

8.3 Zener Diode 1N5333B

The 1N5333B is a Zener diode. As shown in fig. 8.4 the diodes are connected contrariwise for reasons given in section 5.1.2. The rest of the setup is like in the two experiments before.
The voltage peak of the test pulse decreases to a maximum of $U_{res} = 22.5$ V as depicted in fig. 8.5. After a short damped oszillaton it falls to a plateau of 2 V for 6.3 ms.

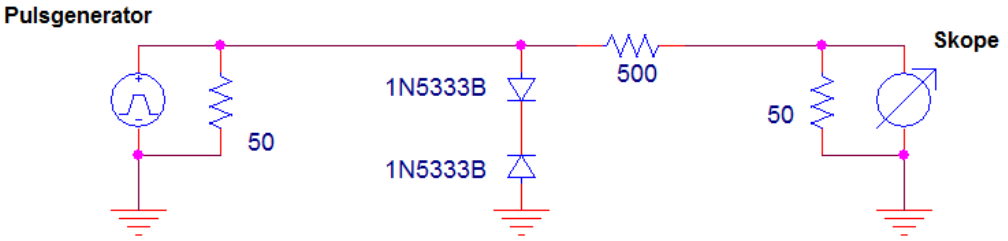

Figure 8.4: test setup for the Zener-diode 1N5333B

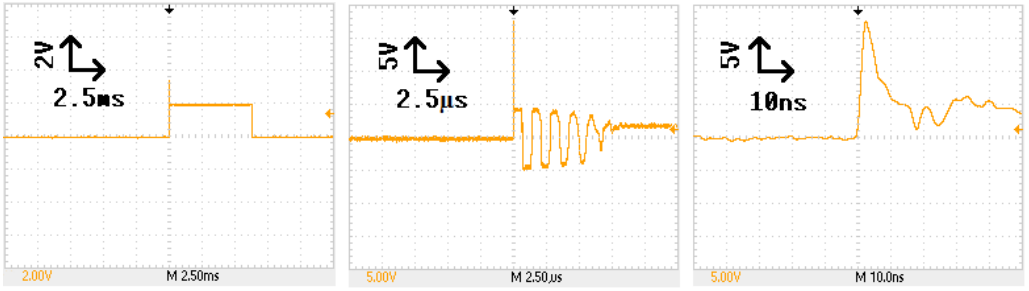

Figure 8.5: The surge pulse damped by two 1N5333B contrarily connected in series. First picture shows the whole pulse. The second and the third show a zoom into the starting peak. The voltage peak decreases to a maximum of $U_{res} = 22.5$ V. After a short damped oszillaton it falls to a plateau of 2 V.

8.4 Schottky Diode 1N5820

The 1N5820 also is a fast switching Schottky diode. It has higher forward voltage of 475 mV. Just slightly higher than at the BAT82, but it has a better power rating so that no additional resistors are needed. The remaining setup is the same as for the BAT82 (see fig. 8.6).
As one can see in fig. 8.7 the voltage is dropped to $U_{res} = 8$ V.

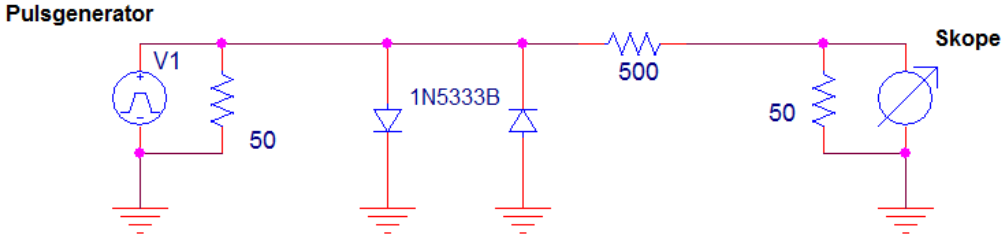

Figure 8.6: Test set-up for the Schottky-diode 1N5820

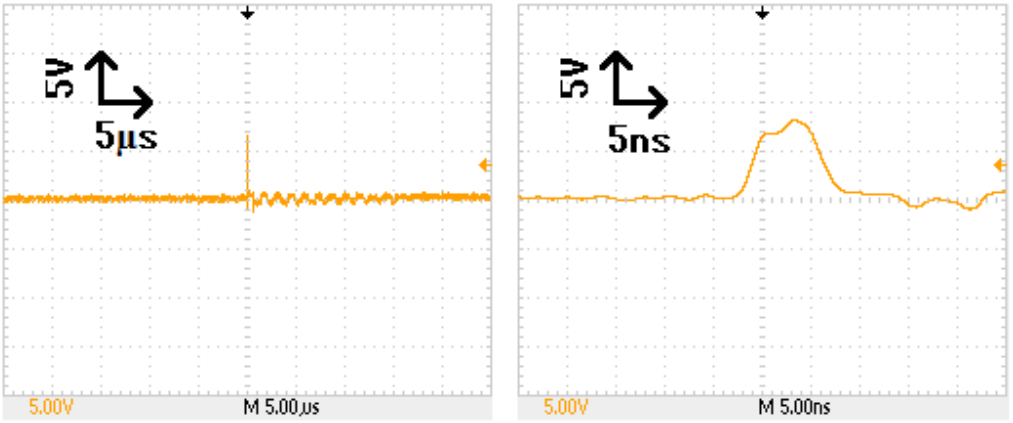

Figure 8.7: The voltage measured with the test setup for 1N5820 as described in fig. 8.6. *Left*: The whole pulse. *Right*: First peak with a higher time resolution.

8.5 Testing Fine and Middle Protection

The experiments in this chapter showed that both the Schottky and the Zener diode potentially are good options for fine protection. Therefore in this section the two diodes with the lowest residual voltage are tested in combination with middle protection.

8.5.1 Zener Diode and GDT

Here, the fine protection consists of two Zener diodes 1N5333B which already were tested in section 8.3. For middle protection the GDT is used. The experiment is set up the same as in chapter 7.1. The only difference is that parallel to the GDT two Zener diodes are contrariwise connected like in fig. 5.2.
Measuring the gain of the amplifier (fig. 8.8) with the FSH4 shows that the LNA works well before the test is carried out.
After firing one 500 V test pulse on the protected amplifier the measurement of the gain shows that the LNA is destroyed, which can be seen in fig. 8.9.

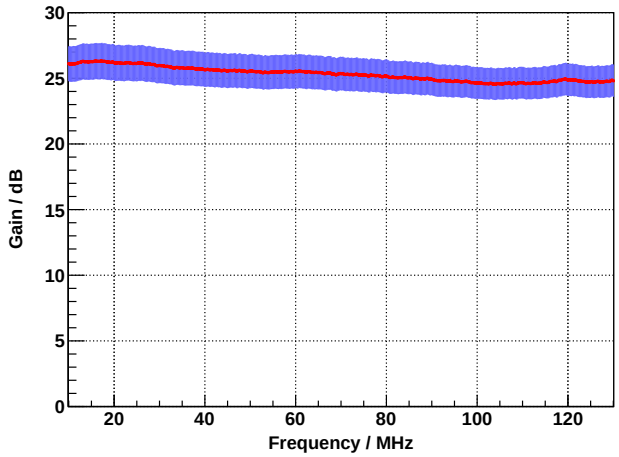

Figure 8.8: *Test-LNA-1*: Gain of a properly working amplifier. Systematical errors in blue.

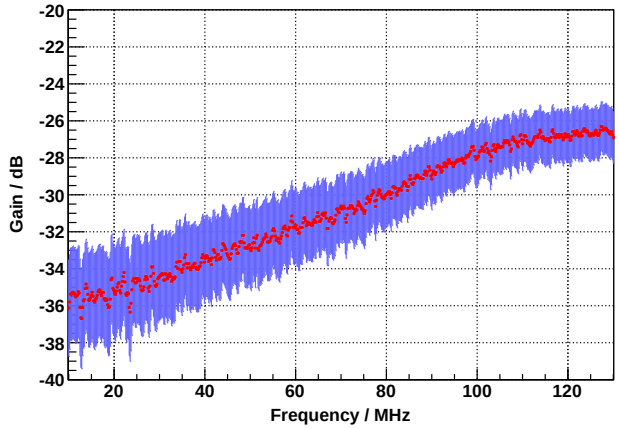

Figure 8.9: *Test-LNA-1* is protected by two Zener diodes 1N5333B contrary connected in series to ground and a GDT (gas discharge tube). The plot shows the gain after firing one 500 V pulse as in fig. 7.1 at its input. The gain is measured without any protection to not falsify the result. Systematical errors in blue.

8.5.2 Schottky Diode and GDT

The Schottky diode 1N5820 possibly is the best option for fine protection. It diverts the 120 V pulse to 8 V which is less than the in chapter 4 fixed lower limit for the maximum permissible voltage U_p.
The test setup is the same as for the Zener diode in section 8.5.1, but instead of the bidirectional Zener diodes here parallel Schottky diodes are applied. Again the gain of the amplifier which can be seen in fig. 8.10 looks reasonable before the test. But, as seen from fig. 8.11 the amplifier breaks when firing the 500 V pulse on it.
Either the residual pulse of the 500 V test puls was higher than 13 V and hence higher than the residual puls of the 120 V puls; or the lower limit for the maximum permissible voltage U_p (see section 4.1) is wrong.

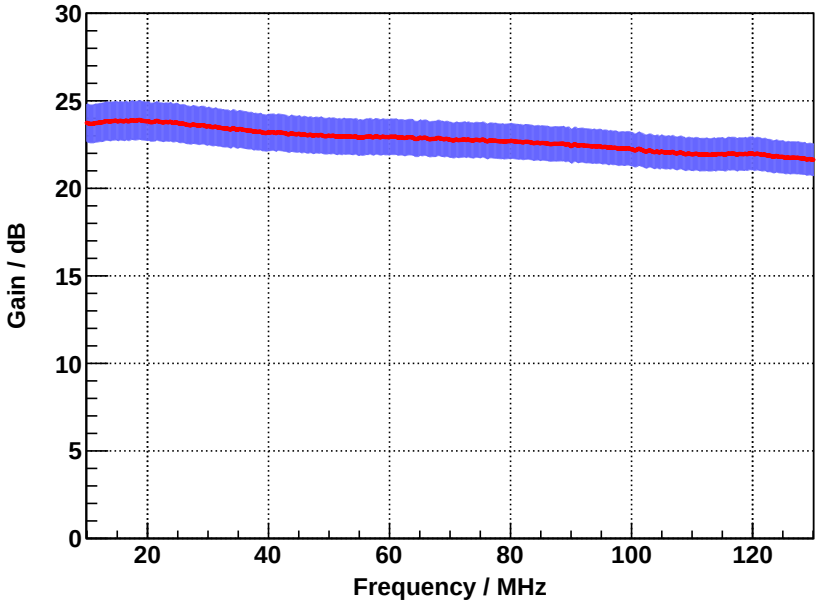

Figure 8.10: *Test-LNA-2*: Gain of a properly working amplifier. Systematical errors in blue.

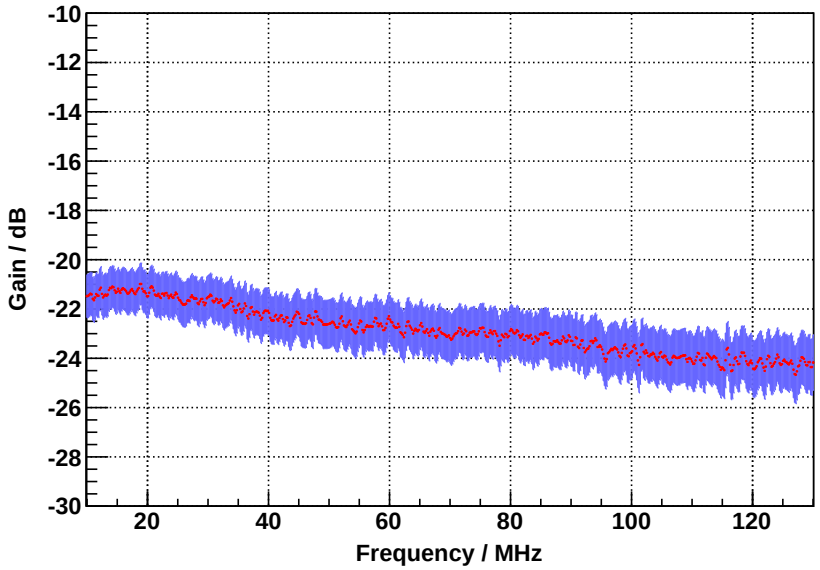

Figure 8.11: *Test-LNA-2* was protected by two Schottky diodes 1N5820 parallel connected to ground and a GDT(gas discharge tube). The plot shows the gain after firing one 500 V pulse as in fig. 7.1 at its input. The gain was measured without any protection to not falsify the result. Systematical errors in blue.

9. Impedance Matching

Chapter 7 and 8 deal with several components of fine and middle protection. More precisely, with their ability to divert surge pulses. Another important criterion for a good lightning protection is that it does not seriously affect the sensitivity of the experiment.
If the impedance of the lightning protection does not match the impedance of the receiving system, reflections can appear. This would sensitively derate the effective gain. The non-negligible high capacitance of the Zener diode is a hint for a bad impedance matching. There is no precise value given in the datasheet but from similar diodes one can assume a value bigger than 1000 pF.
Therefore the reflection factor is measured. When sending a signal the reflection factor is the amount of the signals voltage which is reflected by the input. For this the network analyzer mode of the spectrum analyzer FSH4 from Rohde & Schwarz is used.

9.1 Test of the Impedance Matching

Fig. 9.1 proves that the Zener diode pushes the reflection factor to a totally unacceptable value. In the whole frequency range of interest (30 MHz to 80 MHz) the reflection is more than 70%. This makes the Zener diode 1N5333B unsuitable for protecting the LNA.
The Schottky diode 1N5820 also has a high capacitance. In general the capacitance varies with the frequency and the reverse voltage. At a frequency of 1 MHz and a reverse voltage of less than 1 V the 1N5820 has approximately 500 pF. The measurement of the gain with two parallel connected diodes of this type at the input in fig. 9.2 shows that also this diode has a bad impedance matching to a 50 Ω.

The Schottky diode BAT82, however, has a frequency dependent capacitance of a maximum of 1.8 pF. Here the analyticaly derived reflection factor in the used frequency range is always less than 2.5% as depicted in fig. 9.3. This is an acceptable value for the loss of signal.

9.2 GDT

As seen in section 9.1 a low reflection factor is an important criterion for a good lightning protection system. Here the measurement with the FSH4 (see fig. 9.4) shows that the reflection is less than 2%.
All in all the GDT seems to be a possible option for the middle protection.

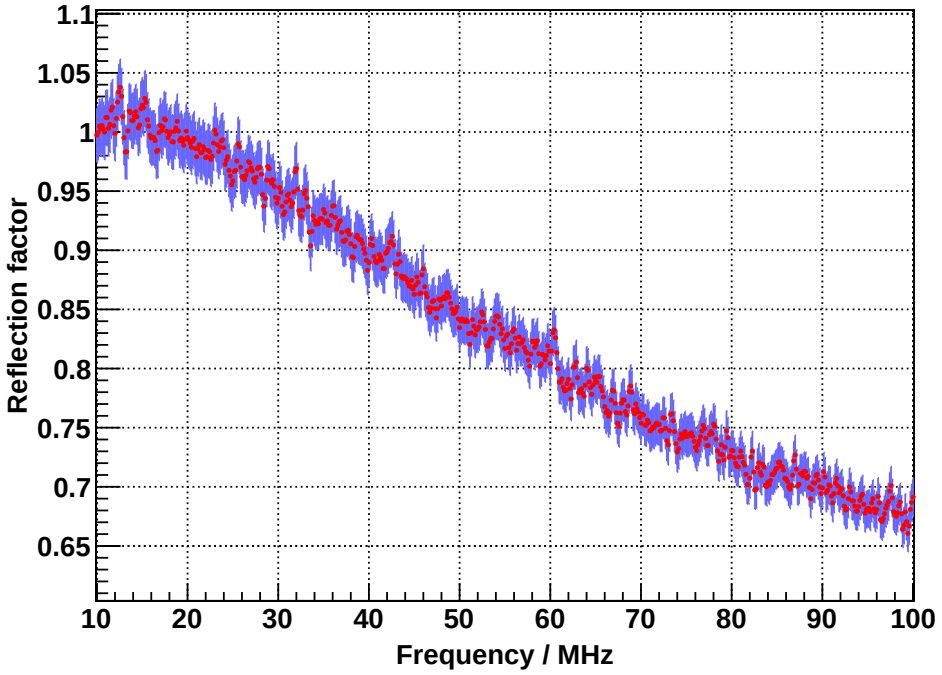

Figure 9.1: Reflection of two bidirectional Zener diodes 1N5333B at a 50 Ω system. For this experiment the diode is connected parallel to the 50 Ω system.

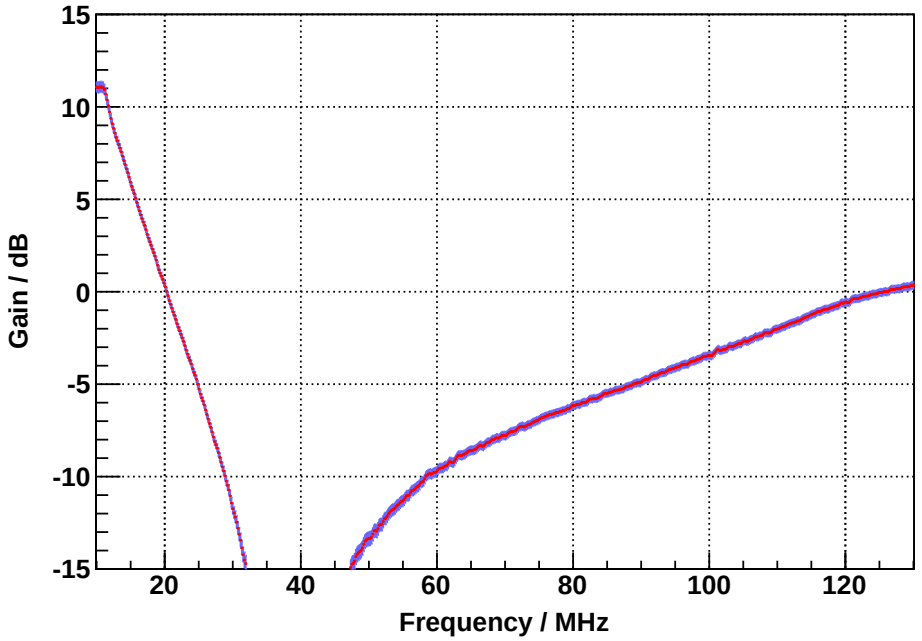

Figure 9.2: The gain of an LNA which is protected by two parallel connected Schottky diodes of the type 1N5820.

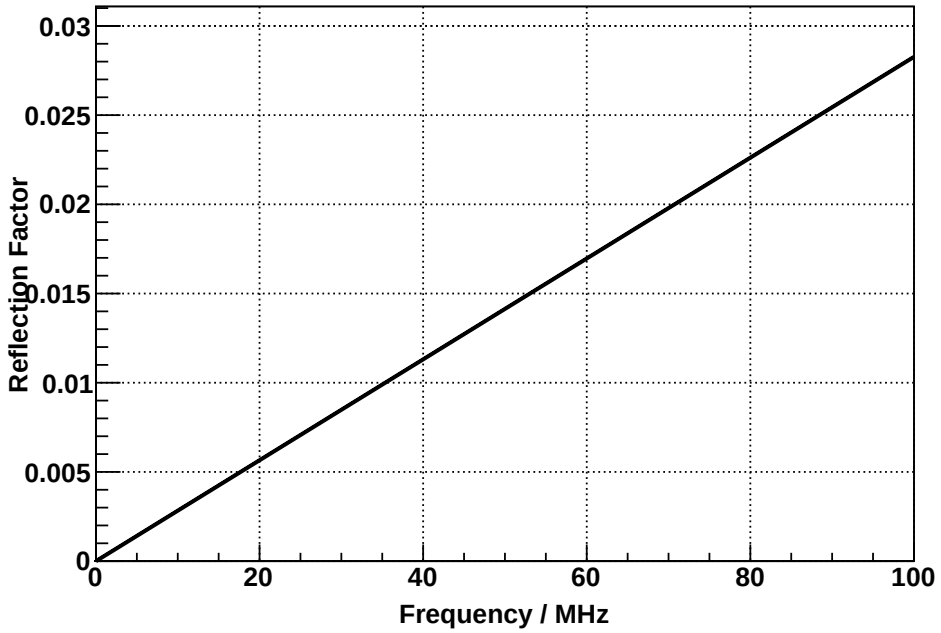

Figure 9.3: The analyticly derived reflection factor of a 1.8 pF capacitance connected to a 50 Ω system

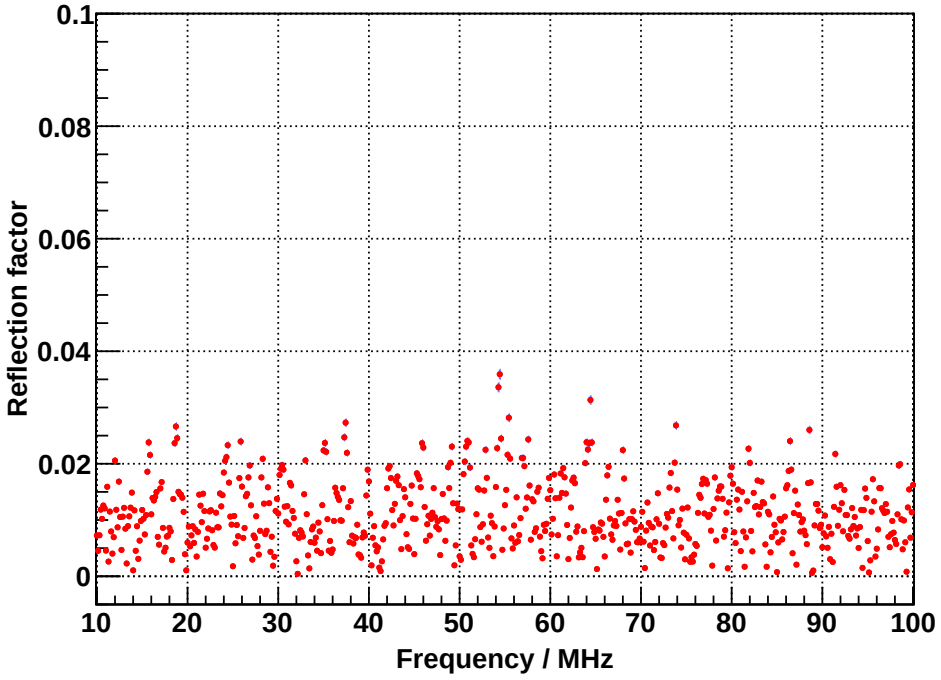

Figure 9.4: The measured reflection factor of the GDT. The Mean= 0.011 ± 0.006.

10. Conclusion and Outlook

The radio detection technique is a promising field of research in the physics of ultra high energy cosmic rays. The Auger Engineering Radio Array (AERA) is a great progress in developing a cost-effective extension for the existing Fluorescence Detector and Surface Detector. As one of its huge advantages is its potential for a high duty cycle, the development of a lightning protection system is defenitely a reasonable effort. It is supposed to keep breakdowns caused by thunderstrom at a minimum level. The first activities in this direction are made in this thesis by developing and testing a protection system for the Low Noise Amplifier (LNA).
Thus, in this work a design for a three-stage-system for overvoltage protection has been introduced, consisting of a fine, middle and coarse protection. The basic idea is to shorten the input of the amplifier when endangered by an overvoltage. The different stages need different voltages to short, so each stage is protected by the next higher stage. The fine protection is the stage which directly protects the LNA. Therefore it has to be very quick. Indeed, the whole lightning protection system should affect the sensitivity of the detector as less as possible.
For the fine protection three different types of diodes were tested, one Zener diode and two Schottky diodes. For the middle protection a Gas Discharge Tube (GDT) was tested. Only the coarse protection was not explicitly tested; but here spark gaps seem to be a good option.
The fine and middle protection were tested with different surge pulses. Additionally the lightning protection was tested at the amplifier itself. The Schottky diode 1N5820 that proved to be the best in diverting voltage. It reduces a 120 V pulse to 8 V. The GDT was tested with a quickly rising 500 V surge pulse. This showed that the response time of the GDT is about 350 ns. After this time the voltage drops to approximate 20 V.
The actual test with the LNA showed that none of the tested diodes in combination with a GDT as middle protection could protect the preamplifier against a 500 V surge pulse. Nevertheless, the GDT works very well at its field of application. It is a good option for middle protection, because 350 ns after the surge pulse starts rising, it takes the largest part of the power away from the fine protection.
Another important criterion is the impedance match of the system. A bad impedance match downgrades the sensitivity of the detector as it causes reflections. Several measurements showed that the diodes which rated to be best in protection have a rather bad impedance match. As rule of thumb one can say that a better ability to divert voltage means higher capacitance which is responsible for the bad impedance match. The GDT, however, has a very good impedance match and re-

flects less than 2 % of the incoming signal.

The main challenge in developing a lightning protection system as introduced in this thesis is to find a diode that solves the conflict between low capacitance and high ability to divert voltage. One thing that should be done first in further research is to determine the exact power rating of the LNA. This will be helpful when searching for a fine protection. And of course, one has to choose and test the devices for the coarse protection.

References

[1] E. A. Grigorov, N.L., *Proc. 12th int. cosmic ray conf. (hobart), 5, 1746*, (1971).

[2] T. A. et al., *Astropart. phys. 24 (2005) 1.*

[3] M. Bertaina, *Proc. of 31th int. cosmic ray conf.*, 2009.

[4] R. A. et al., *Phys. rev. lett. 100 (2008) 101101.*

[5] F. Schüssler, *Proc. of 31th int. cosmic ray conf*, 2009.

[6] The Pierre Auger Collaboration, *The Pierre Auger Collaboration. The Pierre Auger Project TDR. Technical Design Report (unpublished).*

[7] The Pierre Auger Collaboration , *Properties and performance of the prototype instrument for the pierre auger observatory*, Nuclear Instruments and Methods in Physics Research Section A, 518(1-2):172176, (February 2004.).

[8] J. V. Jelley *et al.*, *Radio pulses from extensive cosmic-ray air showers*, Nature, 205:327„ (1965).

[9] T. Huege and H. Falcke, *Radio emission from cosmic ray air showers: Coherent geosynchrotron radiation*, Astronomy & Astrophysics, 412:1934, (2003).

[10] J. D. Jackson, *Classical Electrodynamics. John Wiley & Sons, New York, 2 edition*, 1975.

[11] T. Huege and H. Falcke, *Radio emission from cosmic ray air showers: Monte carlo simulations*, Astronomy & Astrophysics, 430:779-798, (2005).

[12] H. Allan, R. W. Clay, and J. Jones, *Radio pulses from extensive air showers*, Nature, 227:1116-1118, (1970).

[13] R. W. C. H.R. Allan and J. Jones, *Radio pulses from extensive air showers*, Nature, 227:1116-1118, 1970.

[14] T. L. Collaboration, *Progress in air shower radio measurements: Detection of distant events*, Astropart. Phys., 26:332340, (2006).

[15] *Nasa marshall/national space science and technology, center photo release nr: N02-001, http://www.nasa.gov/centers/marshall/home/index.html*, (2002).

[16] P. Hasse and J. Wiesinger, *Handbuch für Blitzschutz und Erdung*, Pflaum Verlag/VDE-Verlag, 1989.

[17] M. Stephan, *Design and test of a low noise amplifier for the auger radio detector*, 2009.

[18] *http://upload.wikimedia.org/wikipedia/commons/thumb/a/a5/diode-iv-curve.svg/2000px-diode-iv-curve.svg.png.*

[19] *http://de.wikipedia.org/wiki/marx-generator.*

Danksagung - Acknowledgements

Zuerst möchte ich mich bei meinem Betreuer Prof. Dr. Thomas Hebbeker bedanken, da er mir die Arbeit an diesem spannenden Thema und einen Einblick in die aktuelle Forschung der Aachener Auger-Arbeitsgruppe ermöglicht hat. Seine wertvollen und interessanten Beiträge haben meine Forschung sehr bereichert.

Ein ganz besonderer Dank gilt Maurice Stephan für seine Unterstützung während der gesamten Arbeit. Die Ergebnisse vieler fruchtbarer Diskussionen mit ihm haben diese Arbeit sehr bereichert und meinen wissenschaftlichen Horizont erweitert.

Dr. Christine Meurer danke ich für die gute Betreuung und Hilfe bei der Planung meiner Arbeit.

Für das Korrekturlesen dieser Arbeit danke ich Dr. Christine Meurer, Maurice Stephan und Lars Mohrmann.

Des weiteren danke ich der ganzen Aachener Auger-Arbeitsgruppe für die freundliche Aufnahme und viele ertragreiche Diskussionen in und auch außerhalb der Meetings. Insbesondere danke ich hier Nils Scharf, der nie müde wurde meine zahlreichen Fragen zu beantworten.

Die Mitarbeiter der elektronischen Werkstatt zeigten stets Interesse an meinen Problemen. Insbesondere möchte ich hier Günter Hilgers und Franz Adamczyk danken. Die Gespäche mit Günter Hilgers haben den Aufbau der Experimente maßgeblich mitbeeinflusst.

Burghart Klein und Martin Janus danke ich für die Leihgabe einer Influenzmaschine.

Des weiteren danke ich Christoph Roggendorf vom Institut für Hochspannungstechnik der RWTH. Der zur Verfügung gestellte Sprunggenerator und unsere Gespräche über Blitzschutz waren für diese Arbeit von großem Nutzen.

Bei Prof. Dr. Joseph Dwyer bedanke ich mich für den hilfreichen Mailverkehr über Blitze und Blitzschutz.

Zum Schluss möchte ich noch ganz besonders meinen Eltern danken, die mich immer unterstützt und mir dieses spannende Studium ermöglicht haben.

Erklärung

Hiermit versichere ich, dass ich diese Arbeit einschließlich beigefügter Zeichnungen, Darstellungen und Tabellen selbstständig angefertigt und keine anderen als die angegebenen Hilfsmittel und Quellen verwendet habe. Alle Stellen, die dem Wortlaut oder dem Sinn nach anderen Werken entnommen sind, habe ich in jedem einzelnen Fall unter genauer Angabe der Quelle deutlich als Entlehnung kenntlich gemacht.

Aachen, den 30. August 2010

Tim Enzweiler